INFLUENCE OF FREEZE-THAW ACTION ON HYDRAULIC BEHAVIOR OF UNSATURATED VOLCANIC COARSE-GRAINED SOILS

Tatsuya Ishikawa[i)], Tetsuya Tokoro[ii)], and Seiichi Miura[iii)]

[i)] Professor, Faculty of Engineering, Hokkaido University, Japan

[ii)] Assistant Professor, Tomakomai National College of Technology, Tomakomai, Japan

[iii)] Professor emeritus, Hokkaido University, Japan

ABSTRACT

This study aims to evaluate the effects of freeze-thaw action on the water retention-permeability characteristics of volcanic coarse-grained soils under unsaturated conditions, in order to examine the hydraulic behavior of volcanic soil during the snow-melting season. In this study, a series of water retention, permeability, and slaking tests on three types of crushable volcanic coarse-grained soils, differing in their degrees of particle crushability, were performed under various degrees of saturation and various freeze-thaw histories, while comparing the test results with those of non-crushable sand. Based on the experimental results, the effects of freeze-thaw action on the water retentivity, permeability, and particle breakage were examined. The test results indicated that freeze-thaw action has strong influence on the hydraulic behavior of crushable volcanic coarse-grained soils under unsaturated conditions, even if the soil is a non-frost-susceptible geomaterial.

Key words: Freeze-thaw testing, Particle breakage, Water retentivity, Permeability, Unsaturated soil, Volcanic coarse-grained soil (IGC: D4/D3/D8)

INTRODUCTION

In cold regions such as Hokkaido, the northern island of Japan, natural disasters such as slope failure on cut slopes or landslides on natural slopes occur often during the snow-melting season. For example, the surface slope failure observed in the snow-melting season is deemed to be caused by an increase in the degree of saturation arising from snow-melting or the change in hydro-mechanical characteristics of soils resulting from freeze-thaw action. Accordingly, it is indispensable to establish a precise method for predicting slope failure in cold regions to examine the influence of freeze-thaw action of pore fluid on the hydro-mechanical behavior of unsaturated soil and to elucidate the mechanism of slope failure observed in cold regions after due consideration of assignments on slope failure in warm-temperate regions where frost heave does not occur.

Moreover, volcanic coarse-grained soils, which are non-frost-susceptible geomaterials widely distributed across Hokkaido, have caused complicated geotechnical engineering problems. This is because volcanic soils possess diverse inherent properties depending on local geology, local topography, and local climate conditions in the depositional environment. The most important property in geotechnical engineering problems is that the mechanical behavior of volcanic coarse-grained soils is greatly affected by the degree of particle breakage (Miura and Yagi 2003). Crushing of volcanic soil particles can be observed even under relatively low stress levels, such as a subsurface layer that has suffered from freeze-thaw action with snowfall and fluctuation in the degree of saturation due to rainfall and/or snow-melting. Ishikawa and Miura (2011) revealed that freeze-thaw action has strong influence on the deformation-strength characteristics of a crushable volcanic coarse-grained soil under saturated conditions because freeze-thaw action produces severe particle breakage during freeze-thawing and shearing. Such singularity in the characteristics of volcanic coarse-grained soils makes it essential to perform studies on this geomaterial.

Accordingly, the influence of freeze-thaw action should be specially considered with regard to surface slope failure on volcanic soils in cold regions in addition to the hydro-mechanical characteristics of unsaturated soils, even if frost heave does not occur. However, synthetic research on disaster prevention measures in Hokkaido lags behind in examining how various factors such as freeze-thaw history, heavy rainfall, and changes in groundwater level individually influence the mechanism of surface slope failure observed on fragmental volcanic soils in the snow-melting season. Synthetic studies on the hydro-mechanical characteristics of unsaturated soils subjected to freeze-thaw action have hardly been seen to date because several non-linear factors influence them interactively.

The objective of this study is to evaluate the effects of freeze-thaw action on the water retention-permeability characteristics of volcanic coarse-grained soils under unsaturated conditions, in order to examine the hydraulic behavior of volcanic soil ground in the snow-melting season. In this study, a series of permeability and water retention tests on two types of crushable volcanic coarse-grained soils, which differ in their degree of particle crushability, are performed under various degrees of saturation and various freeze-thaw histories using test apparatuses for unsaturated soils. The special apparatus used in this study can apply freeze-thaw cycles similar to those experienced by in-situ soils in cold regions to a test specimen. It is also possible to adopt a pressure membrane method for the reduction of total testing time. Based on the experimental results, the effects of freeze-thaw action on water retentivity, permeability, and particle breakage are examined. In addition, a series of slaking tests for the two volcanic coarse-grained soils are performed under various freeze-thaw histories in order to evaluate the effects of both freeze-thaw action and wet-dry cycles on particle crushability and water retentivity of volcanic coarse-grained soils. Based on the experimental results, the dependency of the degree of particle breakage on freeze-thaw action and the influence of change in particle shape and increase in fines content on water retentivity are examined by performing sieve analysis and particle image

analysis.

METHODOLOGY

In this study, a freeze-thaw triaxial apparatus for unsaturated soils (Fig. 1) and a freeze-thaw permeability apparatus for unsaturated soils (Fig. 2) were used. Further information about the apparatuses used in this study were provided previously by Ishikawa et al. (2010).

Freeze-thaw triaxial apparatus

A freeze-thaw triaxial apparatus for unsaturated soils consists of a cooling system to control the temperature of the cap and the pedestal. Therefore, any temperature difference between the cap and the pedestal can be arbitrarily set to the triaxial specimen. Besides, since the specimen is covered with an acrylic cylindrical cell for frost heave simulation during freezing and thawing and the lateral displacement of the specimen is constrained by the cell, one-dimensional frost heave can be replicated in the specimen. Thus, the apparatus can apply a freeze-thaw sequence to a triaxial specimen, as experienced by in-situ soils in cold regions. After the freeze-thaw process, a monotonic triaxial compression test and a water retention test can be performed for coarse-grained soils under various degrees of saturation and loading conditions. In this case, the apparatus can control pore air pressure (u_a) and pore water pressure (u_w) separately. Pore water pressure is applied to the specimen through a hydrophilic acrylic copolymer membrane filter (versapore membrane filter, air entry value (AEV) = 110 kPa) attached to the pedestal, and pore air pressure is applied through a hydrophobic polyflon filter attached to the cap. In addition, axial load can be applied to the specimen in a strain-controlled manner with a direct drive motor. It should be noted that a triaxial compression test can also be performed under saturated conditions by removing the versapore membrane filter on the porous metal.

Freeze-thaw permeability apparatus

A freeze-thaw permeability apparatus for unsaturated soils is an improved permeability apparatus proposed by Ingersoll (1981), Uno et al. (1990), and Abe (1994) with air pressure chambers. This apparatus can perform constant head permeability tests for unsaturated soils by a steady-state method. In order to reduce the total testing time, versapore membrane filters of AEV = 60 kPa and 200 kPa were, respectively, adopted in a water plumbing path and in a measurement path of pore water pressure, rather than using a ceramic plate. On the other hand, a polyflon filter was employed in air supply paths for controlling the pore air pressure. Other key features include the ability to perform water retention tests simultaneously with permeability tests for unsaturated soils by measuring the volume of water inflow and outflow with two electronic force balances installed inside the pressurized chambers. Here, the water supply provides a constant hydraulic head through Mariotte bottles in beakers mounted on electronic force balances. Besides, the apparatus resembles the above-mentioned triaxial apparatus. One-dimensional frost heave observed at in-situ soils in cold regions can be replicated in the specimen just before permeability tests.

TEST SPECIMENS

Soil samples

Four test materials were employed: three volcanic coarse-grained soils (Tomikawa, Kashiwabara, and Touhoro volcanic soils) and Toyoura sand. The volcanic coarse-grained soils were taken from natural deposits in Hokkaido, as shown in Fig. 3. Tomikawa and Kashiwabara volcanic soils belong to the Shikotsu primary tephra deposited by the eruption of the Shikotsu caldera approximately 31,000–34,000 years ago. Touhoro volcanic soil is a fallen pumice stone deposited by the eruption of the Mashu caldera, estimated to have occurred 11,000–13,000 years ago. For reference, Table 1 shows the mineralogical information of the volcanic soil samples. All volcanic soil samples were extracted from depths of over 1.5 m below ground level (lower than the

freezing depths during the twenty years from 1981 to 2000). However, sufficient information is not available on the freeze-thaw history of the samples. Accordingly, in this study, the influence of future freeze-thaw history on the mechanical behavior of all volcanic soils was examined.

The physical properties and grain-size distribution curves of all volcanic soils are shown in Table 2 and Fig. 4, respectively, along with those of Toyoura sand for comparison. All volcanic soils have low values of both maximum and minimum dry densities (ρ_{dmax} and ρ_{dmin}) according to the test method for the minimum and maximum densities of sands (JIS A 1224); this is because their constituent particles are very porous due to the large number of intra-particle voids. As shown in Fig. 4, all volcanic soils characteristically contain coarse and fine fractions, and are coarser than Toyoura sand, although their fines contents (F_c) are as low as 1% and 2%, respectively. Touhoro volcanic soil, in particular, is extremely coarse and well-graded. It is noted that the primary properties of Tomikawa and Kashiwabara volcanic soils are similar in terms of the grain size distribution (Fig. 4) and the mineralogical information (Table 1) because both soils originate from the same eruption (Miura et al. 1996). Furthermore, previous studies (Miura and Yagi 1997; Nakata et al. 1998) have revealed that all volcanic soils exhibit remarkable particle crushability, even under relatively low stress levels. In the range of stress level of tests performed in this study, it is assumed that particle breakage does not occur in Toyoura sand.

Specimen preparation

Volcanic soils obtained from the sampling sites were oven-dried at 110 °C for 24 h and then allowed to cool at an ambient temperature of about 20 °C. A cylindrical specimen was initially 170 mm in height and 70 mm in diameter in the water retention test using the freeze-thaw triaxial apparatus, while a cylindrical specimen was initially 70 mm in diameter and 30 mm in height in the water retention and permeability test using the freeze-thaw permeability apparatus. A specimen was prepared using the air pluviation method with the above-mentioned air-dried

sample (Miura and Toki 1982). Here, to ensure experimental accuracy for the ratio of maximum particle size versus specimen diameter, the particles of grain size above 9.5 mm and 4.75 mm were screened from the original volcanic soil samples while preparing the specimens for the freeze-thaw triaxial apparatus and the freeze-thaw permeability apparatus, respectively. The initial dry densities of the specimens (ρ_{d0}) were adjusted by changing the drop height of sample such that the dry density after consolidation (ρ_{dc}) would be equal to the in-situ dry density ($\rho_{din\text{-}situ}$), as shown in Table 2. Allowable variations in ρ_{dc} were limited to within ±5% of the prescribed density. As for Toyoura sand, a cylindrical specimen was also prepared using the air pluviation method with an air-dried sample such that the initial relative densities of the specimens (D_r) would be equal to D_r = 82%. The initial relative densities of all the volcanic soils are less than that of Toyoura sand.

EXPERIMENTAL PROGRAMS

In this study, water retention and permeability tests were mainly performed on unsaturated volcanic coarse-grained soils before and after freeze-thaw action, as follows:

Freeze-thawing water retention test

a) Freeze-thaw process

In accordance with the "Test method for frost heave prediction of soils (JGS 0171-2003)," the following freeze-thaw process was conducted: First, an acrylic cylindrical cell for one-dimensional frost heave was installed on a soil specimen enclosed in a rubber membrane, and de-aired water was added from the bottom end of the specimen for around three hours until the degree of saturation was at least 80% (Hereafter, the state of the specimen after water permeation will be referred to as "quasi-saturation"). Next, the specimen was one-dimensionally consolidated by loading a weight corresponding to the axial stress (σ_a) of 12.2 kPa on the top of the specimen, in consideration of the overburden pressure acting on the subsurface layer. Subsequently, the

specimen was frozen from the upper part and thawed from the lower part with a cooling system while allowing unfrozen water in the specimen to inflow and outflow through a water plumbing path of the pedestal due to frost heave and thaw settlement of the specimen (open-system freezing). Here, the temperature gradient throughout the specimen was maintained at 0.1 °C/mm, and the constant freezing (cooling) and thawing rate (u) was 1.6 °C/h. In this study, the above-mentioned series of operations was defined as 1 freeze-thaw cycle. After the freeze-thaw process, the cell for frost heave was removed from the specimen. Ishikawa and Miura (2011) is referred for detailed information about testing methods applied in this study.

b) Consolidation process

Before beginning a water retention test, the quasi-saturated specimen was isotropically consolidated under a prescribed net normal stress (σ_{net}) of 49.0 kPa in a fully drained condition by applying a prescribed confining pressure (σ_{c}) of 249 kPa, pore air pressure (u_a) of 200 kPa, and pore water pressure (u_w) of 200 kPa until there was no longer a tendency for the changes in the axial displacement or the drainage volume. Here, the net normal stress (σ_{net}) is defined as $\sigma_{\mathrm{net}} = \sigma_{\mathrm{c}} - u_a$.

c) Water retention process

After the consolidation process, a water retention test was commenced under a condition near saturation, and it proceeded through a drying process in accordance with the following procedure. The axis-translation technique was adopted to set an intended matric suction (s) on the drying curve; this was achieved by decreasing u_w while keeping both σ_{c} and u_a constant. Here, matric suction (s) is defined as $s = u_a - u_w$. Upon attaining an equilibrium condition (i.e., when outflow of water from the specimen has stopped), the water content corresponding to the applied matric suction was computed by reading the change in water volume between two successive applied suctions with a double tube burette. The above-described procedure was then repeated for higher values of matric suction by decreasing the applied pore-water pressures incrementally until the

drying curve of the soil-water characteristic curve (SWCC) was complete. After the drying process, the test continued with the wetting process. Matric suction (s) was reduced by increasing the applied pore water pressure. A decrease in matric suction (s) caused water to flow from the plumbing path back into the soil specimen. Following equilibrium, the change in water content was measured under incrementally decreasing matric suction (s). The procedure was repeated at different matric suctions until the desired range of the wetting curve was obtained. For comparison, a water retention test for a non-freeze-thawed specimen was also performed under the same experimental conditions.

Freeze-thawing permeability test on unsaturated soils

a) Freeze-thaw and consolidation processes

Similarly to the above-mentioned freeze-thaw process in the freeze-thawing water retention test, a freeze-thaw test of the quasi-saturated specimen was conducted one-dimensionally with open-system freezing, which allowed water inflow/outflow from the specimen during freeze-thawing. It is noted that the temperature gradient throughout the specimen was maintained at 0.2 °C/mm. Subsequently, a quasi-saturated specimen was isotropically consolidated under a prescribed net normal stress (σ_{net}) of 49.0 kPa in a fully drained condition similarly to the above-mentioned consolidation process in the freeze-thawing water retention test.

b) Permeability and water retention processes

After the freeze-thaw and consolidation processes, constant head permeability tests were performed at a condition near saturation, where the matric suction was close to zero and the tests proceeded through a drying process in accordance with the following procedure. First, the steady-state method for measuring the coefficient of permeability (k_w) was performed by applying a constant hydraulic head difference of about 1.0 cm between the pedestal and the cap under a constant net normal stress (σ_{net}) of 49 kPa. The constant hydraulic gradient (i) in the vertical

direction yielded one-dimensional steady-state seepage from the pedestal to the cap across the specimen. Steady-state seepage conditions were achieved when the inflow rate (ΔQ_{in}) of water to the specimen and the outflow rate (ΔQ_{out}) of water from the specimen were equal, as shown in Eq. 1:

$$\Delta Q = \Delta Q_{\text{in}} = \Delta Q_{\text{out}} \tag{1}$$

where ΔQ is the volume of water per unit time. Both ΔQ_{in} and ΔQ_{out} are computed using the volume of water (Q) flowing across the specimen in a designated time period (t), which is measured using electronic force balances. It is noted that the water supply and the drainage are given positive signs of ΔQ_{in} and ΔQ_{out}, respectively. The coefficient of permeability (k_w) can be computed as

$$k_w = \frac{\Delta Q}{iA} = \frac{\Delta Q}{A} \cdot \frac{L}{\Delta h} \tag{2}$$

where i is the hydraulic gradient in the range of 0.4 to 0.9, A is the cross-sectional area of the seepage path, L is the height of the specimen, and Δh is the head loss across the specimen and is measured with a differential pressure gauge connected to both the cap and pedestal. The above-described experimental procedure was repeated for different magnitudes of matric suction or water content by decreasing the applied pore water pressure (u_w) incrementally while maintaining both σ_c and u_a constant, i.e., while maintaining a constant net normal stress (σ_{net}). Moreover, the volume of water inflow and outflow during each increment of matric suction was measured with electronic force balances, and they were used in calculating the water contents of the specimen, thereby yielding the water retention curve and permeability coefficients from a single soil specimen.

Particle size analysis

Before and after testing, particle size analysis was performed for all tested specimens to assess

the degree of particle breakage that occurred throughout the test. The degree of particle breakage was measured in terms of the increment of fines content (ΔF_c), which is the change between the fines content of the sheared and the original specimen (Nakata et al. 1998). The fines content (F_c) is simply the percent finer corresponding to a grain size of 0.075 mm diameter in its particle size distribution curve, as shown in Fig. 5. It is noted that the sieve analysis was performed with due care so as not to induce any new particle breakage.

Freeze-thawing slaking test

In order to evaluate the effects of cyclic freeze-thaw action and wet-dry cycles on the physical properties of crushable granular materials, two slaking tests with different freeze-thaw histories were newly proposed with reference to the "Method for rock slaking test (JGS2124-2006)," and were performed with Tomikawa and Touhoro volcanic soils. A cylindrical specimen inside a thin-walled tube was prepared by the air pluviation method with an oven-dried test sample, as shown in Fig. 6. The initial dry densities of specimens (ρ_{d0}) were calculated to be almost equal to the in-situ dry densities (Table 2).

The freeze-thawing slaking test was carried out in the following four steps (Fig. 7): (1) an immersion process of the specimen in water at room temperature of 20 °C for 24 h, (2) a freezing process of the specimen in a freezer at -20 °C for 24 h, (3) a thawing process of the specimen in water at room temperature for 24 h, and (4) a gravity drainage process of the specimen in air at room temperature for 24 h. On the other hand, a slaking test without freeze-thaw sequences was carried out through the following two steps: (1) an immersion process of the specimen in water at room temperature for 72 h and (2) a gravity drainage process of the specimen in air at the room temperature for 24 h. It is noted that the testing time of the immersion process in the slaking test was set at 72 h in conformity with the total testing time of the first three processes in the freeze-thawing slaking test. Furthermore, the slaking tests proposed in this study differ in the freeze-

thaw history and the testing time for the immersion process mentioned in "Method for rock slaking test (JGS 2124-2006)." For information, little difference was noticed in the results of slaking tests under different immersion process testing times, according to the preliminary results of both volcanic soils.

In this study, the above-mentioned series was defined as 1 cycle, and 5 cycles were repeatedly applied to the specimens because the change in the deformation-strength characteristics of Tomokawa and Touhoro volcanic soils caused by repeated freeze-thaw actions converged at around the number of freeze-thaw cycles (N_f) of 5 (Ishikawa and Miura 2011). After each cycle, the water content (w) of the specimen was measured and particle size analysis was performed for the specimen to assess the degree of particle breakage during the test. In addition, a photograph of the particle shape was separately taken for some same soil particles after each cycle (Fig. 8).

Image analysis of particle shape

After converting the cross-section of soil particles shot with a digital camera into X-Y coordinate values, the particle shape of the volcanic coarse-grained soils was evaluated by two analytical methods, which used either the argument or the radius function (Kono et al. 2000). The argument function is a function of the tangential line at P_x, which is the point advanced x from the reference point S, and the angle of reference line θ(x), as shown in Fig. 9. If the perimeter of the particle is L, the argument function is normalized as shown in Eq. 3, since $\theta(x+L) = \theta(x) + 2\pi$:

$$\theta_{N(x)} = \theta_{(x)} - 2\pi(x/L) \tag{3}$$

where θ_N(x) is the normalized argument function. Since the normalized argument function θ_N(x) is a periodic function of period L, it can be developed into a Fourier series, as shown in Eq. 4. The k-th amplitude spectrum can be expressed by Eq. 5:

$$\theta_{N(x)} = b_0/2 + \sum_{k=1}^{\infty}\{a_k \sin(2\pi kx/L) + b_k \cos(2\pi kx)/L\} \tag{4}$$

$$C_k = \sqrt{a_k^2 + b_k^2} \tag{5}$$

where a_k and b_k are

$$a_k = (2/L)\int_{x_0}^{x_0+L} f(x)\sin(2\pi kx/L)dx \qquad \text{k=1, 2,}\cdots$$

$$b_k = (2/L)\int_{x_0}^{x_0+L} f(x)\cos(2\pi kx/L)dx \qquad \text{k=1, 2,}\cdots \tag{6}$$

Kono et al. (2000) reported that the sum of the 3rd to 20th amplitude spectra in Eq. 6 indicates the degree of the angularity of the particle. Hence, this study assumed that the angularity of a particle shape was defined by the normalized argument function value (NA_{fv}), as given in Eq. 7:

$$NA_{\mathrm{fv}} = \sum_{k=3}^{20} C_k \tag{7}$$

On the other hand, the radius function is a function of the length $r(\alpha)$ of the straight line that connects a certain point P_α on the contour and the center of gravity O, as shown in Fig. 9. This is expressed by Eq. 8. The k-th amplitude spectrum is expressed by Eq. 9:

$$r_{(\alpha)} = b_0/2 + \sum_{k=1}^{\infty}\{a_k \sin(k\alpha) + b_k \cos(k\alpha)\} \tag{8}$$

$$C_k = \sqrt{a_k^2 + b_k^2} \tag{9}$$

where a_k and b_k are

$$a_k = (1/\pi)\int_{\alpha_0}^{\alpha_0+2\pi} r(\alpha)\sin(k\alpha)d\alpha \qquad \text{k=1, 2,}\cdots$$

$$b_k = (1/\pi)\int_{\alpha_0}^{\alpha_0+2\pi} r(\alpha)\cos(k\alpha)d\alpha \qquad \text{k=1, 2,}\cdots \tag{10}$$

Kono et al. (2000) reported that the ratio of the second- and zeroth-order amplitude spectra shown

in Eq. 9 indicates the degree of the aspect ratio of the particle. Then, the variation in the aspect ratio was defined by the radius function value (R_{fv}), as given in Eq. 11:

$$R_{fv} = C_2 / C_0 \quad \text{k=1, 2,}\cdots \tag{11}$$

Furthermore, in this study, the change in the intra-particle void of the volcanic coarse-grained soils was investigated using micro-focus X-ray computed tomography (CT) to clarify the influence of freeze-thaw action on the microstructure in a nondestructive manner. A micro-focus X-ray CT scanner with a maximum spatial resolution of 5 μm was used. Other properties of the micro-focus X-ray CT scanner were explained in the study of Fukuda et al. (2012). The X-ray CT scanning was applied to a soil particle before and after freeze-thaw. A soil particle was dried for a day at room temperature before each X-ray CT observation to remove water from the particle. Observations were conducted after the above-mentioned immersion process and after the freeze-thaw process. For one soil particle of each volcanic soil, six CT slice images were obtained to calculate the intra-particle void ratio (e_{ip}). In this study, e_{ip} is defined as the ratio of the area of intra-particle void to the area of soil material (Table 3). The particle sizes for Tomikawa and Touhoro volcanic soils were about 4 mm and 7 mm in height, respectively.

RESULTS AND DISCUSSIONS

Behavior of soil specimens during freeze-thaw process

According to Ishikawa and Miura (2011), the frost heave could hardly be recognized in the volcanic soil samples, while a small settlement was observed after thawing and the density increased. The thaw settlement of volcanic coarse-grained soils is considered to be caused by particle breakage due to freeze-thaw action. For example, when the freeze-thaw process is repeated, the average grain size (D_{50}) of volcanic soils decreases with the increment of particle breakage, as shown in Fig. 10. Besides, both dry density after the freeze-thaw process (ρ_{df}) and increment in fines content (ΔF_c) increase with the number of freeze-thaw cycles (N_f), although the

rates of increase gradually decrease with increasing N_f for the second and subsequent times (Fig. 11). These results indicate that a distinct amount of particle breakage is caused by cyclic freeze-thaw action in crushable volcanic coarse-grained soils, even for non-frost-susceptible geomaterials, and that the particle breakage causes a volumetric contraction of soil specimens and the transformation of the particle skeleton into a denser structure than before.

Effect of freeze-thaw action on SWCC

First discussion is on the difference in the water retentivity of crushable volcanic coarse-grained soil and non-crushable sand. Figs. 12 and 13 show SWCCs during the drying process and the wetting process of a freeze-thawed specimen and a non-freeze-thawed specimen in water retention tests for Tomikawa volcanic soil and Toyoura sand. It is noted that the SWCCs in Figs. 12 and 13 were obtained from the water retention tests with the freeze-thaw triaxial apparatus. The plot for both the freeze-thawed specimen and the non-freeze-thawed specimen shows the hysteresis effect between the drying and wetting curves. As for Tomikawa volcanic soil, matric suction (s) arises in the specimen at a high water content (around S_r = 70%), and increases sharply with decreasing degree of saturation (S_r). However, even if matric suction increases in the range over 60 kPa, the degree of saturation tends to converge at a specific value, namely a residual degree of saturation (S_{r0}), of about S_{r0} = 25% for non-freeze-thawed specimen and 30% for freeze-thawed ones. Such SWCCs of Tomikawa volcanic soil differ from those of Toyoura sand in that the boundary effect area and the air entry values are not recognized clearly at low suction ranges, irrespective of the freeze-thaw history. Moreover, the whole range of matric suction in Tomikawa volcanic soil is higher than that in Toyoura sand, and the difference can be considered to be caused by the difference in fines content between both soil samples, as shown in Table 2.

Next, the effects of the freeze-thaw history on the water retention curves of both soil samples are discussed. As for Toyoura sand, the difference in SWCCs between a freeze-thawed

specimen and a non-freeze-thawed specimen can hardly be recognized because the dry densities before and after consolidation are nearly equal and the grain size distributions remain unchanged regardless of the presence or absence of a freeze-thaw process. Conversely, for plots with the same degree of saturation in Tomikawa volcanic soil, matric suction (s), namely the water retentivity of a freeze-thawed specimen during the drying process, increases in comparison with that of a non-freeze-thawed one, although the shape of the SWCCs remains almost unchanged. As the freeze-thaw process is repeated, the location of the SWCC gradually shifts to the right because the fines content increases with the number of freeze-thaw cycles (N_f), as shown in Fig. 11, thereby changing the grain size distribution. Fredlund et al. (1997) reports variation of the SWCC arising from changes in grain size distribution, and Zapata et al. (2000) showed that, for non-plastic soils, the SWCC can be estimated from the grain diameter (D_{60}) corresponding to 60% passing in the grain size distribution curve, and that the larger the value of D_{60} is, the lower the water retentivity. The above-mentioned experimental results of this study are in fair agreement with these past studies.

The reason seems to be due to the grain-refining of crushable volcanic soils mainly caused by freeze-thaw, which ultimately results in a gradual increase in the water retentivity of the soil. Accordingly, for Toyoura sand, no particle breakage occurred due to freeze-thaw action, which led to a little change in the water retentivity and permeability before and after freeze-thawing. Incidentally, the reason why the above-mentioned difference is not observed in the wetting portion of the SWCCs in Tomikawa volcanic soil is that the starting points on the wetting curves varied with the individual test in Fig. 12. These results indicate that freeze-thaw action has a strong influence on the water retention characteristics of crushable volcanic soils, even though they are referred as non-frost-heaving geomaterials.

Effect of freeze-thaw action and wet-dry cycles on physical properties of volcanic soils

Fig. 14 shows the relations of both water content ratio (w/w_0) and the increment in the fines content (ΔF_c) (which were obtained from two slaking tests with and without freeze-thaw cycles for Tomikawa and Touhoro volcanic soils) to the number of cycles (N_c) for freeze-thawing and slaking. Here, the water content ratio (w/w_0) is the ratio of the water content (w) at any given N_c to the water content (w_0) at $N_c = 0$.

For Tomikawa volcanic soil, both w/w_0 and ΔF_c increase with N_c regardless of the presence or absence of freeze-thaw cycles. On the other hand, for Touhoro volcanic soil, although ΔF_c increases with N_c regardless of the presence or absence of freeze-thaw sequences, the trend of w/w_0 differs from that for Tomikawa volcanic soil. For example, w/w_0 decreases with increasing wet-dry cycles in slaking tests without freeze-thaw sequences, while, in freeze-thawing slaking tests, it initially increases and decreases from around $N_c = 3$ cycles by the combined actions of freeze-thawing and wetting and drying. Furthermore, for both volcanic soils, freeze-thaw action significantly influence the change in w/w_0 and ΔF_c as compared with the effects of wet-dry cycles, and the difference in the trends between the two slaking tests becomes more pronounced with an increase in N_c.

Nakata and Miura (2007) revealed that the number of intra-particle voids with an opening ("opened intra-particle void" in Fig. 15) can be estimated using the water content after gravity drainage for 24 h. Given the results obtained in this study, it seems reasonable to consider that one of the reasons for the rise in the water retentivity of crushable volcanic coarse-grained soils is that cyclic freeze-thawing and/or cyclic wetting and drying result in a gradual increase in the amount of opened intra-particle voids associated with a triggering of particle breakage. Besides, since the fines content increases along with N_c, an increase in water retentivity is expected. However, as shown in Fig. 14, the water retentivity of Touhoro volcanic soil decreases by freeze-thaw action and wet-dry cycles. This phenomenon will be examined in a later section.

Effect of freeze-thaw action and wet-dry cycles on change in particle shape

Fig. 16 shows the relation of the normalized argument function value ratio (NA_{fv}/NA_{fv0}) to the number of cycles (N_c) for freeze-thawing and slaking for Tomikawa and Touhoro volcanic soils. Here, the normalized argument function value ratio (NA_{fv}/NA_{fv0}) is the ratio of the normalized argument function value (NA_{fv}) at any given N_c to the one at $N_c = 0$.

For Tomikawa volcanic soil, NA_{fv}/NA_{fv0} increases with N_c, regardless of the presence or absence of freeze-thaw sequences, whereas, for Touhoro volcanic soil, NA_{fv}/NA_{fv0} decreases with increasing wet-dry cycles at slaking tests without freeze-thaw sequences, and initially increases and decreases from around $N_c = 3$ cycles at freeze-thawing slaking tests. These trends of NA_{fv}/NA_{fv0} with N_c agree well with those of w/w_0, as shown in Fig. 14, irrespective of the soil samples. On the other hand, the significant correlation of w/w_0 and the radius function value (R_{fv}) was hardly recognized from the results of image analysis of particle shapes using the radius function, which showed that the R_{fv} value was almost constant even though the freeze-thawing and wetting and drying were repeated. In general, the normalized argument function value is considered to be an effective index for evaluating the angularity of soil particles, while the radius function value is considered to be an effective index for the sphericity. Accordingly, Fig. 16 shows that the particle shape of Tomikawa volcanic soil becomes angular by freeze-thaw action and/or wet-dry cycles, while the particle shape of Touhoro volcanic soil becomes curved with N_c increase as seen in Fig. 8. It is noted that Tomikawa volcanic soil is a representative air-fall pyroclast in Japan, namely primary tephra. This particle has not experienced natural selection, and on this account, the particle shape is angular. These results also indicate that the decrease in the angularity of soil particles is closely related to the decrease in water retentivity. Moreover, considering the fact that the overall particle shape, like the aspect ratio, is hardly altered by freeze-thawing and wetting and drying, the change in the angularity of soil particles is considered to mainly arise from the disappearance of the irregularity on a particle surface.

Incidentally, a phenomenon whereby the water retentivity of Touhoro volcanic soil decreases by freeze-thaw action and/or wet-dry cycles can be explained from the viewpoint of the change in particle shape. It is considered that though this micro phenomenon is not experimentally proved, some closed intra-particle voids initially turn into opened intra-particle voids due to freeze-thaw action in freeze-thawing slaking tests for Touhoro volcanic soil, as shown in Fig. 17, thereby increasing the water retentivity. However, after the generation of new opened intra-particle voids converges at around N_c = 3 cycles, the water retentivity gradually drops along with the decrease in the angularity associated with the commencement of particle breakage. On the other hand, in the slaking without freeze-thaw sequences, few opened intra-particle voids are newly generated, and cyclic wetting and drying seems to result in a continued decrease in water retentivity. In addition, the water retentivities of the two volcanic coarse-grained soils differ from each other due to particle crushability. Since Tomikawa volcanic soil exhibits low particle crushability as compared with Touhoro volcanic soil (Fig. 14), it is considered that the transition from closed intra-particle voids to opened intra-particle voids by freeze-thaw action hardly occurs in Tomikawa volcanic soil, and that the decrease in the angularity of soil particles due to freeze-thawing and wetting and drying is not so significant. Consequently, the increase in the fines content and angularity of the soil particles caused by repeated freeze-thawing and continuous wetting and drying have heightened the water retentivity of Tomikawa volcanic soil.

Finally, the results of X-ray CT observations for soil particles (Fig. 18) are examined to investigate the influence of freeze-thaw action on the microstructure of crushable volcanic coarse-grained soils. In Fig. 18, a part with dark color inside the particle exhibits the intra-particle void. It is recognized that Tomikawa volcanic soil and Touhoro volcanic soil have many intra-particle voids. Table 3 shows the intra-particle void ratios (e_{ip}) of both volcanic soils before and after freeze-thawing. Comparing the e_{ip} values of both volcanic soils, Tomikawa volcanic soil has

larger intra-particle void than Touhoro volcanic soil, and the freeze-thaw action increases the intra-particle void irrespective of the soil sample. However, the analytical result showing that a larger difference in the intra-particle void before and after freeze-thawing is seen in Tomikawa volcanic soil disagrees with the discussions in the preceding paragraph. This is because the discussions on the e_{ip} value mainly focus on the change in not opened intra-particle voids but closed intra-particle voids inside a soil particle. In addition, the transition from closed intra-particle voids to opened intra-particle voids by freeze-thaw action could hardly be discerned in the results of X-ray CT observations for soil particles. Therefore, the influence of freeze-thaw action on the microstructure, including both opened and closed intra-particle voids of crushable volcanic coarse-grained soils, needs to be further investigated.

Effects of freeze-thaw action on hydraulic behavior

Fig. 19 shows the SWCCs obtained from the permeability tests along drying processes on Kashiwabara and Touhoro volcanic soils with different freeze-thaw histories. Fig. 20 compares the relations of the coefficient of permeability (k_w) to the degree of saturation (S_r) and matric suction (s), obtained from the same tests as those shown in Fig. 19. It should be noted that the results in Figs. 19 and 20 were obtained from the water retention and permeability tests with the freeze-thaw permeability apparatus. For the plots with the same degree of saturation (S_r) in Fig. 19, as for volcanic coarse-grained soils, matric suction (s) of a freeze-thawed specimen increases in comparison with that of the non-freeze-thawed one, though the shape of the SWCCs with unclear air-entry values remains almost unchanged irrespective of the soil sample. These trends of the water retention and permeability tests for Kashiwabara volcanic soil agree well with those of the above-mentioned water retention tests for Tomikawa volcanic soil (Fig. 12), even though the maximum grain size is different from each other. However, when comparing Figs. 12 and 19 under the same matric suction, the degree of saturation of Kashiwabara volcanic soil with the

maximum grain size (D_{max}) of 4.75 mm is higher than that of Tomikawa volcanic soil with D_{max} of 9.5 mm irrespective of the freeze-thaw history, although the Kashiwabara and Tomikawa volcanic soils have similar primary properties except the grain size distribution. Furthermore, the effect of the freeze-thaw action on the water retention characteristics of volcanic coarse-grained soil varies depending on the soil type and the grain size distribution, or the fines content before the test. These indicate that the comprehensive comparison between both the test results will serve the qualitative evaluation of the water retention-permeability characteristics for crushable volcanic coarse-grained soils subjected to freeze-thaw action, while the quantitative evaluation needs the accumulation of further experimental results.

On the other hand, for the plots with the same degree of saturation (S_r) in Fig. 20a, the coefficient of permeability (k_w) of a freeze-thawed specimen decreased in comparison with that of the non-freeze-thawed one, though the coefficient of permeability decreased with the decrease in degree of saturation (S_r) as expected, regardless of freeze-thaw history. According to Fredlund et al. (2012), when the coefficient of permeability is cross-plotted against the volumetric water content, there is essentially no hysteresis between the drying and wetting curves. Contrarily, Sugii et al. (2002) demonstrated that when the dry density or the void ratio of soils varies significantly, the unsaturated coefficient of permeability also changes, in addition to the change in the SWCC. Taking these past achievements into account, it is considered that the increase in the dry density of volcanic coarse-grained soils due to freeze-thaw action, as mentioned above, causes a change in the k_w–S_r relation. However, as shown in Fig. 20b, the freeze-thaw history has little influence on the decreasing tendency of k_w with matric suction, in contrast with the effect on the SWCC. For each volcanic soil, the relation seems to be approximated as a curve with a slight dispersion regardless of the presence or absence of a freeze-thaw process, as shown in Fig 20b. These results indicate that matric suction has a stronger influence on the water permeability characteristics of crushable volcanic coarse-grained soils as compared with the change in particle skeleton structure

caused by particle breakage, and that if the SWCCs of volcanic coarse-grained soils with different freeze-thaw histories are known, the unsaturated permeability of volcanic coarse-grained soils can be estimated using the k_w–s relation given in Fig. 20b. However, there is room for further investigation of the validity of the above-mentioned tendencies in a higher suction range.

Fig. 21 summarizes the influence of freeze-thaw action on the water retention-permeability characteristics of crushable volcanic coarse-grained soils under unsaturated conditions, which have been revealed in this study. This figure indicates that under the real in-situ conditions, where the constant pore water pressure due to the specified groundwater level is applied at atmospheric pressure (namely under the constant matric suction), the freeze-thaw action induces an increase in the fines content due to particle breakage on the fragmental volcanic soil ground, thereby leading to a rise in the water retentivity while keeping the hydraulic conductivity constant. In general, slope failure due to rainfall in warm-temperate regions is mainly caused by the following exogenous factors: a) increase in weight of soil mass; b) decrease in the suction of unsaturated soil with increase in water content; and c) increase in pore water pressure with increase in groundwater level and seepage pressure (Kitamura and Sako 2010). By contrast, as shown in Fig. 21, on a fragmental volcanic soil ground in cold regions, the increase in the unit weight of the soil and the change in the water retention-permeability characteristics followed by particle breakage owing to freeze-thawing may lead to a slope failure during the thawing season. For example, in the case of rapid snow-melting caused by a sharp air-temperature rise and/or heavy rainfall during the thawing season on a fragmental volcanic soil slope, the water retentivity of the soil increases and the permeability decreases due to freeze-thaw action; this leads to the inhibition of water migration within the subsurface layer, an increase in the unit weight of the soil and pore water pressure, and a decrease in the shear strength, thereby indicating an increased tendency for slope failure. Therefore, when constructing new roads and railroads on fragmental volcanic soil ground in cold regions, sufficient attention should be paid to the

influence of the freeze-thaw action on the stability of the embankment and/or the cut slope in terms of design and maintenance, in addition to the exogenous factors of slope failure in warm-temperate regions.

CONCLUSIONS

The following findings are obtained from the present study:

- Particle breakage of volcanic coarse-grained soils increases due to freeze-thaw action and wet-dry cycles, even though they are non-frost-susceptible geomaterials, and this particle breakage causes the volumetric contraction of soil specimens and the transformation of the particle skeleton into a denser structure than before.
- Grain refining of the volcanic soil particles due to freeze-thaw cycles results in a gradual increase in water retentivity. With an increase in the number of freeze-thaw cycles, the difference in the SWCCs between a freeze-thawed specimen and a non-freeze-thawed specimen becomes remarkable. However, the effect of the freeze-thaw action on the SWCCs varies depending on the soil type and the grain size distribution.
- Shape change with the grain refining of volcanic soil particles due to cyclic freeze-thawing and/or cyclic wetting and drying causes a gradual fluctuation in water retentivity because it is considered that freeze-thaw action and wet-dry cycles give rise to a gradual increase in the amount of opened intra-particle voids associated with the commencement of particle breakage although this phenomenon could not be sufficiently proved by the results of X-ray CT observations for soil particles in this study.
- Matric suction has a stronger influence on the permeability characteristics of crushable volcanic coarse-grained soils as compared with the change in particle skeleton structure caused by particle breakage. Accordingly, if the SWCCs of volcanic coarse-grained soils with different freeze-thaw histories are known, the unsaturated permeability of volcanic

coarse-grained soils can be estimated using the unique relation between the coefficient of permeability and matric suction.

From the findings of this study, it seems reasonable to conclude that freeze-thaw action has strong influence on the hydraulic behavior of crushable volcanic coarse-grained soils under unsaturated conditions, even if the soil is a non-frost-susceptible geomaterial. Therefore, this study clarifies that even on fragmental volcanic coarse-grained soil ground, where frost heave does not occur, evaluation of the effect of freeze-thaw history on the slope stability from the viewpoint of particle breakage is essential for establishing a precise predictive method of natural disasters in cold regions. However, further investigation on the influence of freeze-thaw actions on the deformation-strength characteristics of unsaturated volcanic coarse-grained soil is needed to elucidate the failure mechanism of volcanic soil slopes in cold regions.

ACKNOWLEDGMENTS

This research was supported in part by the Committee on Advanced Road Technology of the Ministry of Land, Infrastructure, Transport and Tourism, Japan, and Grant-in-Aid for Scientific Research (A) (19201035) and Grant-in-Aids for Scientific Research (B) (16310121 & 23360201) from the Japan Society for the Promotion of Science (JSPS) KAKENHI.

REFERENCES

Abe, H. (1994): Experimental study on the estimation of mechanical properties for unsaturated soils, *Ph.D. Thesis*, University of Tokyo, Tokyo. (in Japanese)

Fredlund M.D., Fredlund D.G., and Wilson G.W. (1997): Prediction of the soil-water characteristic curve from grain-size distribution and volume-mass properties, *Proceedings of 3rd Brazilian symposium on Unsaturated Soils*, Rio de Janeiro, April 22-25, 1997: 1-12.

Fredlund D.G., Rahardjo H., and Fredlund M.D. (2012): Unsaturated Soil Mechanics in

Engineering Practice, *John Wiley & Sons, Inc.*: 336-339.

Fukuda, D., Nara, Y., Kobayashi, Y., Maruyama, M., Koketsu, M., Hayashi, D., Ogawa, H., and Kaneko, K. (2012): Investigation of self-sealing in high-strength and ultra-low-permeability concrete in water using micro-focus X-ray CT, *Cem. Concr. Res*. 42: 1494-1500.

Ingersol, J.E. (1981): Method for coincidentally determining soil hydraulic conductivity and moisture retention characteristics, *Special Report*, **81-2**, U.S. Army Cold Regions Res. and Eng. Lab., Hanover, NH.

Ishikawa, T. and Miura, S. (2011): Influence of freeze-thaw action on deformation-strength characteristics and particle crushability of volcanic coarse-grained soils, *Soils and Foundations*, **51**(5): 785-799.

Ishikawa, T., Tokoro, T., Ito, K. and Miura, S. (2010): Testing methods for hydro-mechanical characteristics of unsaturated soils subjected to one-dimensional freeze-thaw action, *Soils and Foundations*, **50**(3): 431-440.

Japanese Geotechnical Society (2003): Test method for frost heave prediction of soils (JGS 0171-2003), *Standards of Japanese Geotechnical Society for Laboratory Soil Testing Methods*, 39-44.

Japanese Geotechnical Society (2006): Method for rock slaking test (JGS 2124-2006), *Japanese standards and explanations of laboratory testing and investigation methods for rock*: 35-38.

Japanese Standards Association (ed.) 2009. Test method for minimum and maximum densities of sands (JIS A 1224: 2009). Japanese Industrial Standards. (in Japanese).

Kitamura R., and Sako T. (2010): Contribution of "Soils and Foundations" to studies on rainfall-induced slope failure, *Soils and Foundations*, **50**(6): 955-964.

Kono, A., Sekine, E. and Kohata, Y. (2000): A study on shape evaluation method of granular material. In A. R. Dawson (ed.), *Unbound Aggregates in Road Constuction UNBAR5*, Proc.

intern. symp., Nottingham, 21-23 June, 2000: 35-40.

Machida, Y. and Arai, F. (2003): *Atlas of tephra in and around Japan (revised edition)*, Univ. of Tokyo Press, Tokyo, 284p. (in Japanese)

Miura, S. and Toki, S. (1982): A sample preparation method and its effect on static and cyclic deformation-strength properties of sand, *Soils and Foundations*, **22**(1): 61-77.

Miura, S. and Yagi, K. (1997): Particle breakage of volcanic coarse-grained soils and its evaluation, *Journal of Geotechnical Engineering*, 561/III-38, 257-269. (in Japanese)

Miura, S. and Yagi, K. (2003): Mechanical behaviour and particle crushing of volcanic coarse-grained soils in Japan, In Tan, et al. (eds), *Characterisation and Engineering Properties of Natural Soils*, Proc. Intern. Workshop, Singapore, 2-4 December 2002: 1169-1203.

Miura, S., Yagi, K. and Kawamura, S. (1996): Static and cyclic shear behavior and particle crushing of volcanic coarse grained soils in Hokkaido, *Journal of Geotechnical Engineering*, **547**/III-36, 159-170. (in Japanese).

Nakata, T. and Miura, S. (2007): Change in void structure due to particle breakage of volcanic coarse grained soil and its evaluation, *Journal of Geotechnical Engineering*, **63**(1): 224-236. (in Japanese).

Nakata, T., Miura, S. and Kawamura, S. (1998): Particle breakage and its evaluation of volcanic coarse-grained soils, Yanagisawa et al. (eds), *Problematic Soils IS-TOHOKU'98*, Proc. Intern. Symp., Sendai, 28-30 October 1998: 145-148.

Sugii T., Yamada K., and Kondou T. (2002): Relationship between soil-water characteristic curve and void ratio, *Proceedings of the 3rd Intern. Conf. on Unsaturated Soils, UNSAT2002*, Recife, March 10-13, 2002: 209-214.

Uno, T., Sato, T., Sugii, T. and Tsuge, H. (1990): Method of test for permeability of unsaturated sandy soil with controlled air pressure, *Journal of Geotechnical Engineering*, **418**/III-13, 115-124. (in Japanese).

Zapata, C.E., Houston, W.N., Houston, S.L and Walsh, K.D. (2000): Soil-water characteristic curve variability, In Shackelford C. D. et al. (eds), *Advances in Unsaturated Geotechnics*, Proc. Sessions of Geo-Denver 2000, Denver, 5-8 August 2000: 84-123.

Table 1. Mineralogical information of volcanic soil samples (after Machida and Arai, 2003)

Name of sample	Major mineral[a]	Main component of volcanic glass[b]								
		SiO_2 (%)	TiO_2 (%)	Al_2O_3 (%)	FeO (%)	MnO (%)	MgO (%)	CaO (%)	Na_2O (%)	K_2O (%)
Tomikawa (Spfa-1)	opx, cpx, ho, qt	77.5	0.2	13.1	1.4	0.0	0.4	1.4	3.5	2.6
Kashiwabara (Spfa-1)	opx, cpx, ho, qt	78.6	0.2	12.5	1.4	0.1	0.1	1.2	3.4	2.6
Touhoro (Ma-1)	opx, cpx	–	–	–	–	–	–	–	–	–

[a] opx : orthorhombic pyroxene, cpx : monopyroxene clinoaugite, ho : hornblende, qt : quartz.

[b] No data on main component of volcanic glass for Touhoro volcanic soil.

Table 2. Physical properties of samples

Name of sample (USCS soil classification)	Soil particle density ρ_s	Maximum dry density ρ_{dmax}[a]	Minimum dry density ρ_{dmin}[a]	In-situ dry density $\rho_{din\text{-}situ}$	Mean grain size D_{50}	Uniformity coefficient U_c	Initial fines content $F_{c,\,initial}$
	(g/cm^3)	(g/cm^3)	(g/cm^3)	(g/cm^3)	(mm)		(%)
Tomikawa volcanic soil (SP)	2.22	0.522	0.426	0.490	1.10	3.32	1.00
Kashiwabara volcanic soil (SP)	2.34	0.623	0.462	0.530	1.25	3.50	0.90
Touhoro volcanic soil (SW)	2.44	0.680	0.483	0.500	5.00	7.08	1.97
Toyoura sand (SP)	2.65	1.648	1.354	–	0.18	1.59	0.00

[a] Results determined by JIS A 1224: 2009.

Table 3. Change in intra-particle void by X-ray CT observation

Name of sample	Intra-particle void ratio, e_{ip}	
	before freeze-thaw	after freeze-thaw
Tomikawa volcanic	0.303	0.320
Touhoro volcanic soil	0.175	0.176

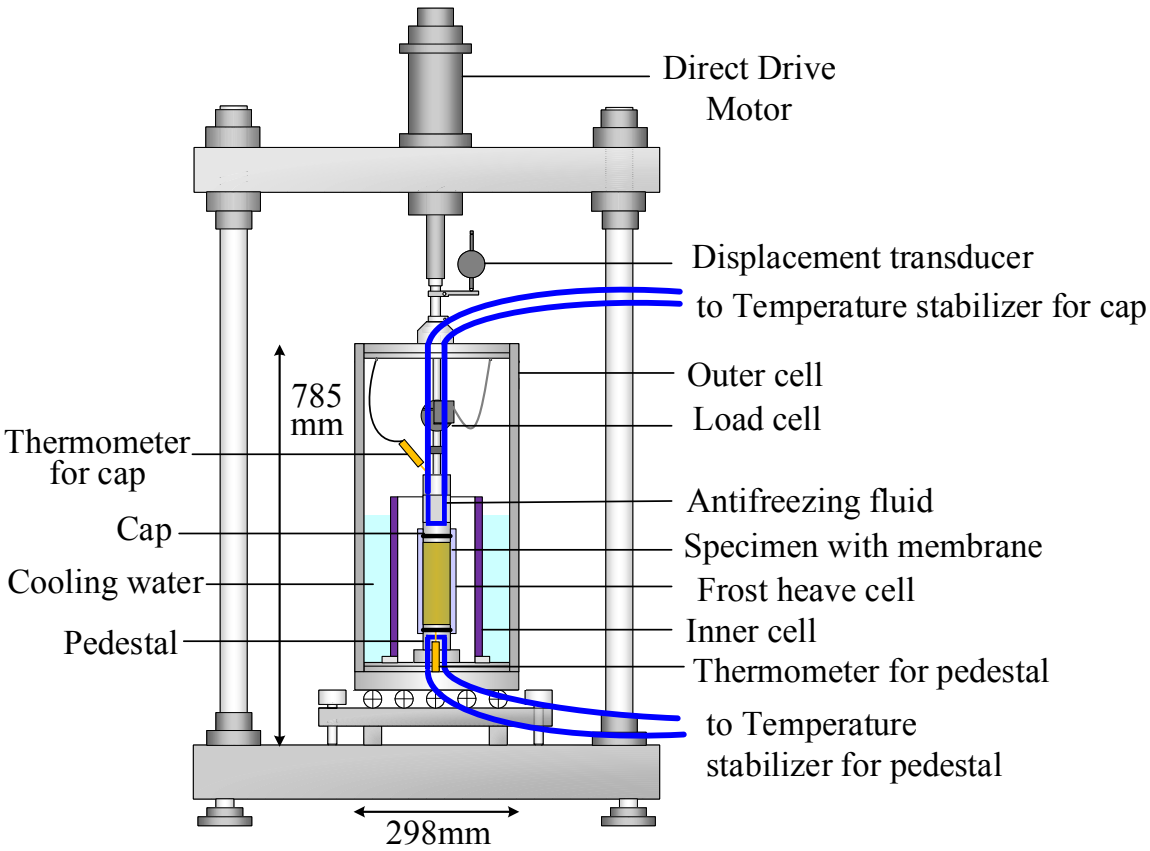

(a) Schematic diagram

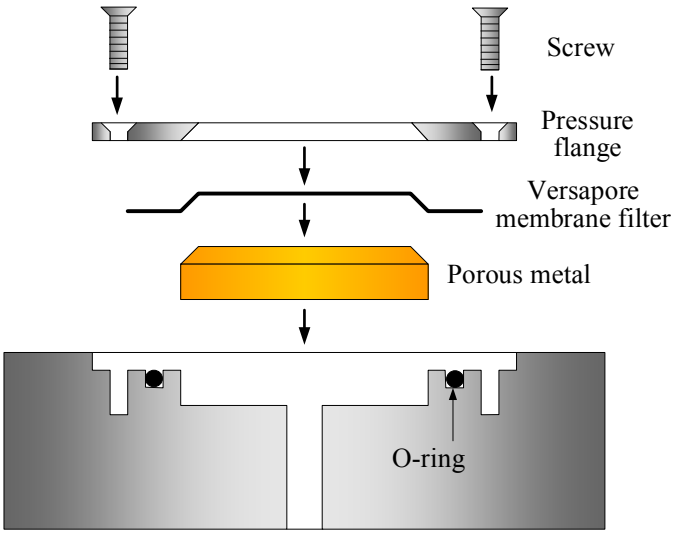

(b) Structure of pedestal

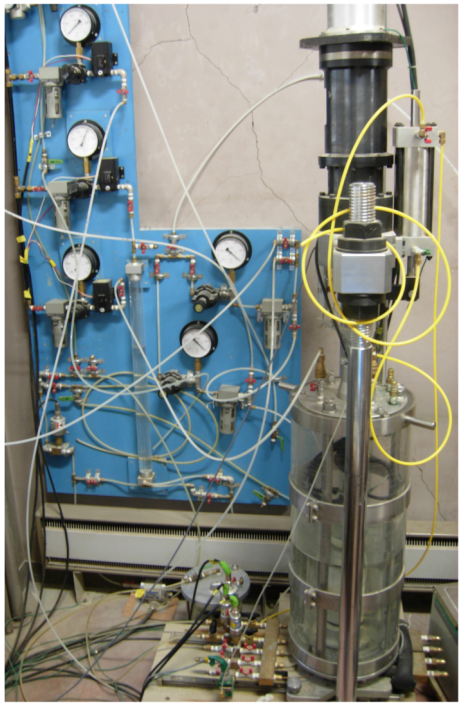

(c) Photo

Fig. 1. Freeze-thaw triaxial apparatus (after Ishikawa and Miura, 2011)

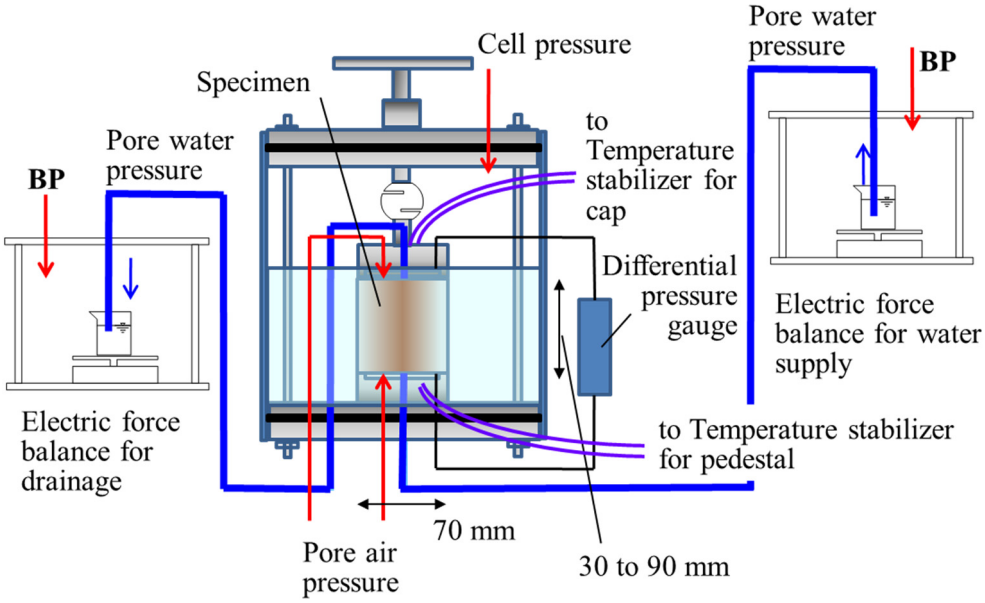

(a) Schematic diagram

(b) Photo

Fig. 2. Freeze-thaw permeability apparatus

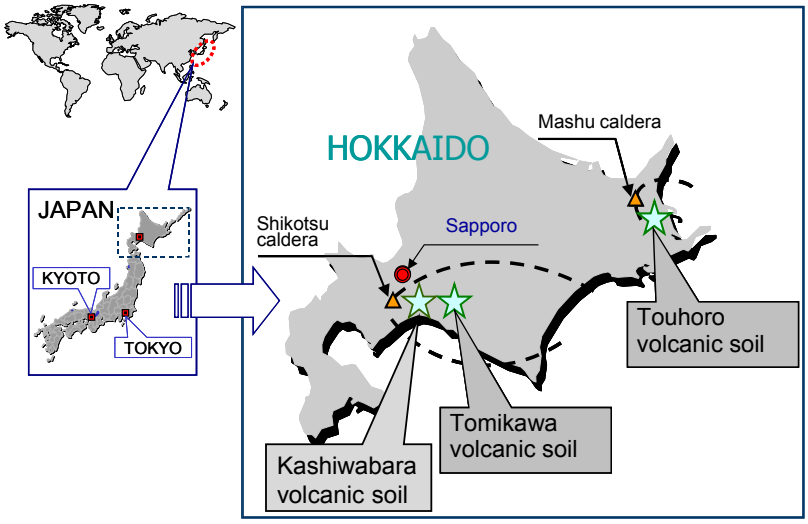

Fig. 3. Sampling sites of volcanic soils

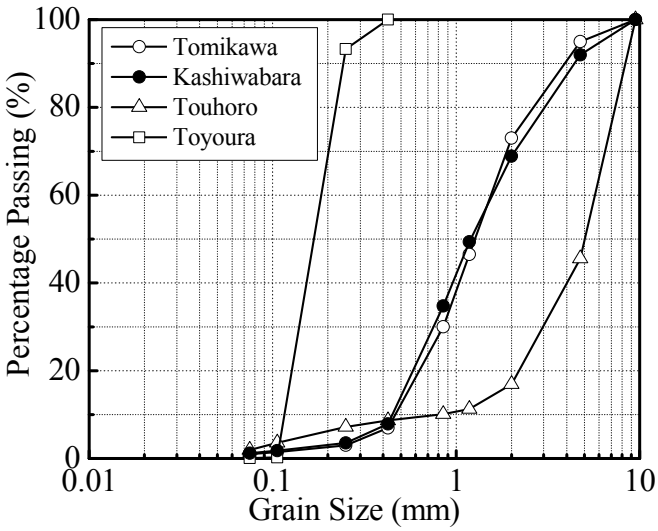

Fig. 4. Grain-size distribution curves of samples

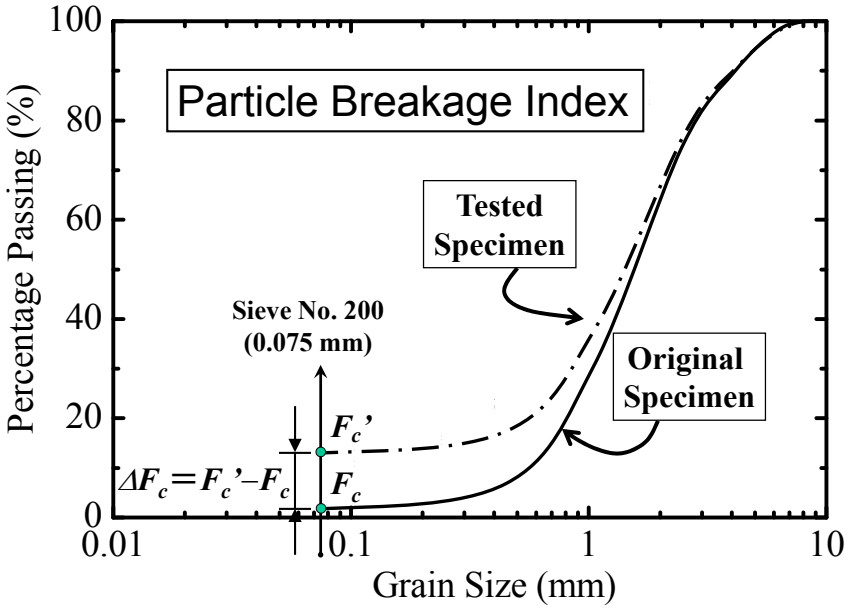

Fig. 5. Definition of particle breakage index, ΔF_c

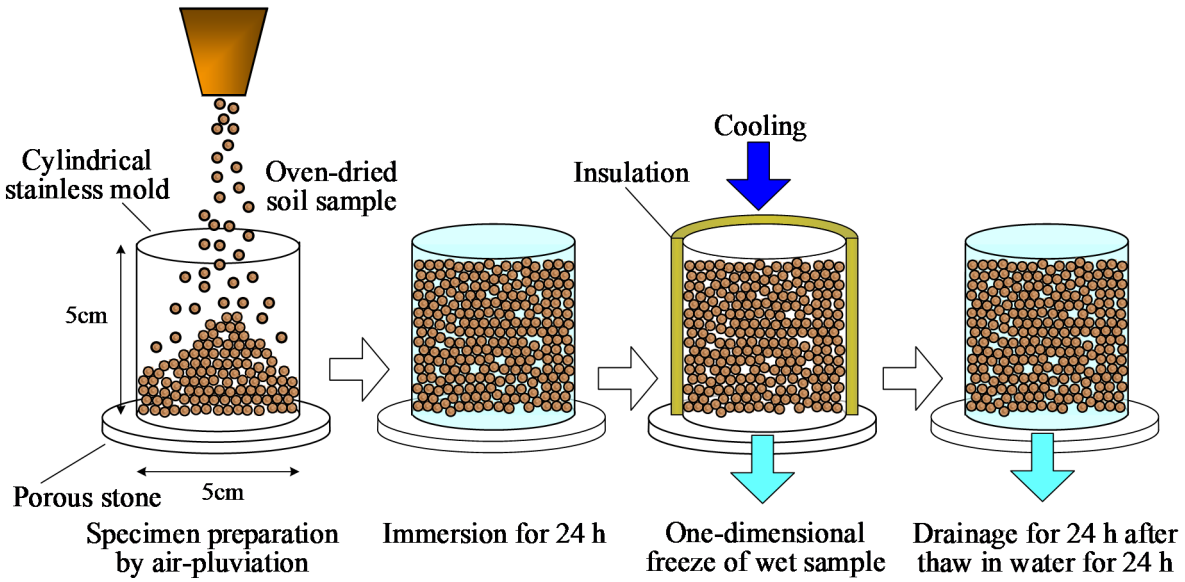

Fig. 6. Test procedures of freeze-thawing slaking test

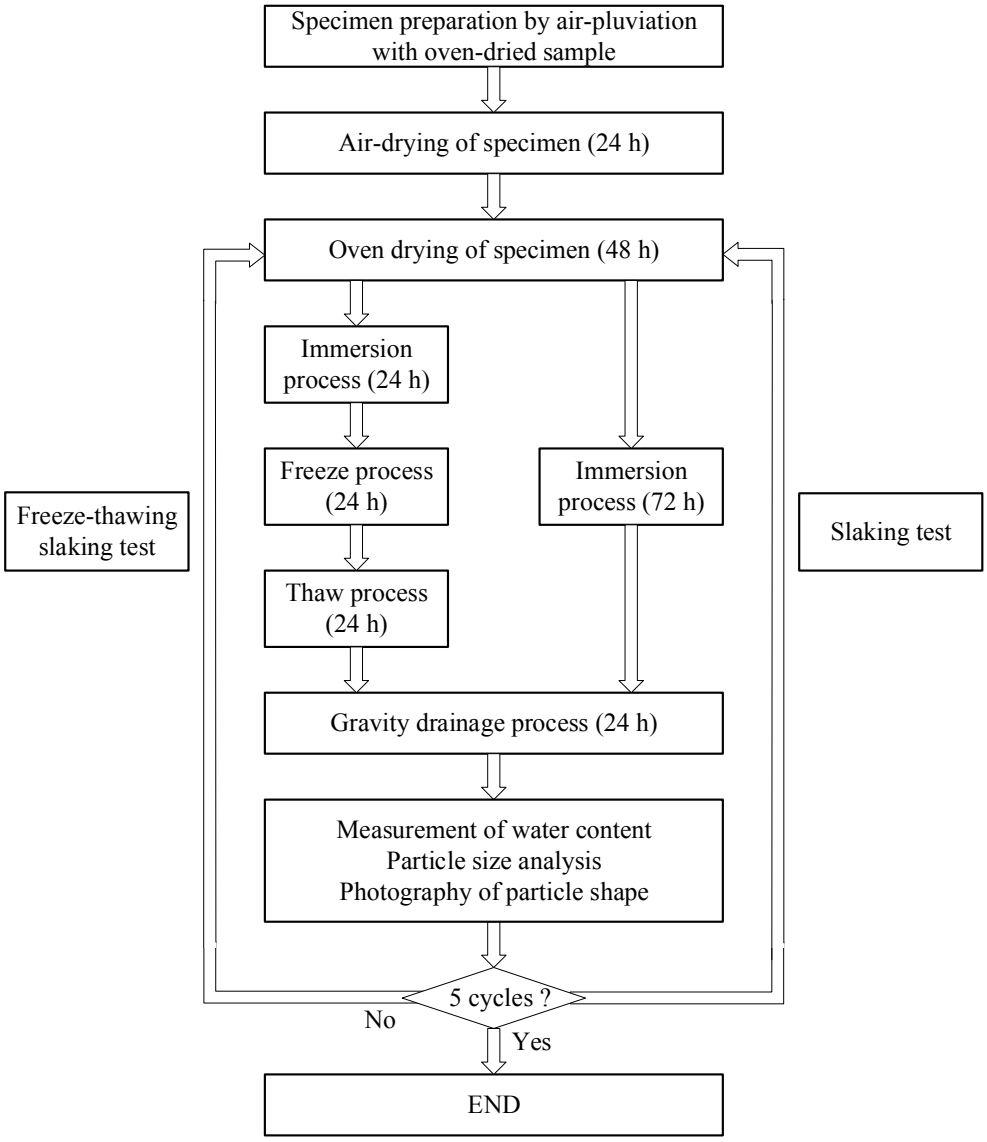

Fig. 7. Testing method of freeze-thawing slaking test

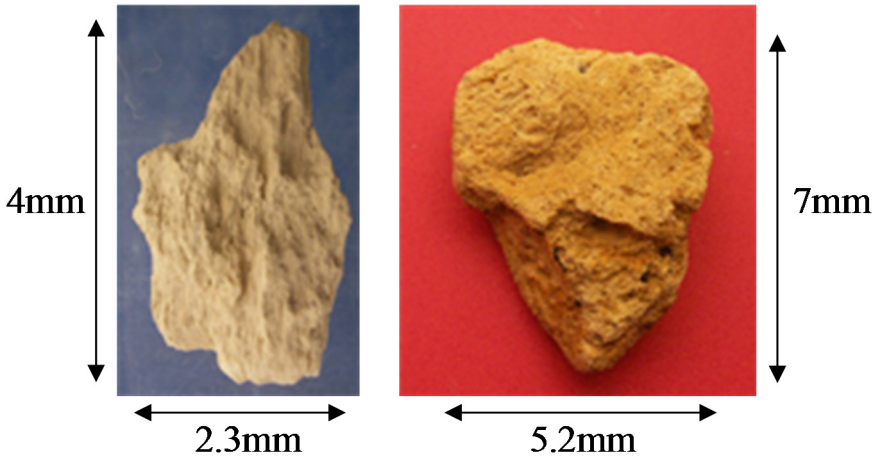

(a) Before freeze-thawing slaking test

(b) After freeze-thawing slaking test (5 cycles)

Fig. 8. Photos of volcanic soil particles (Left: Tomikawa volcanic soil, Right: Touhoro volcanic soil)

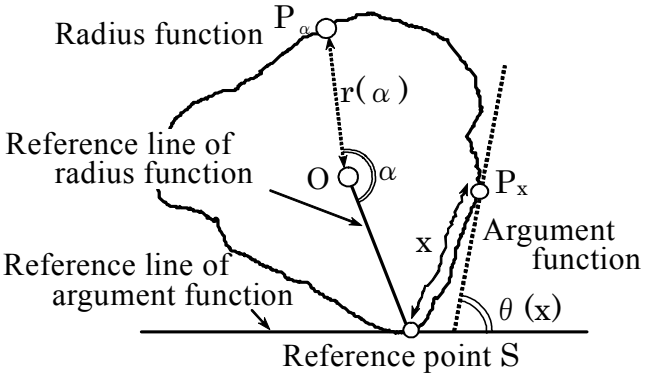

Fig. 9. Conceptual figure of argument and radius function (after Kono et al., 2000)

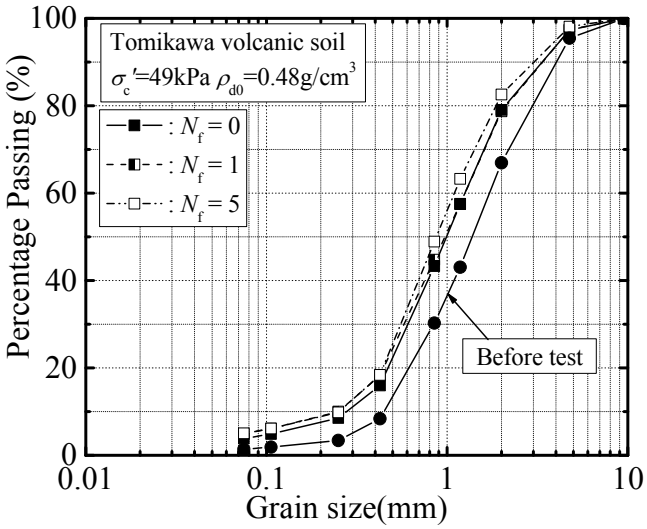

(a) Tomikawa volcanic soil

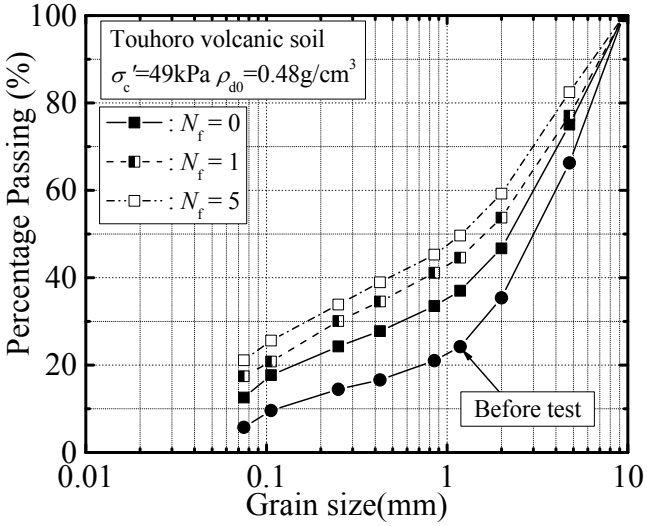

(b) Touhoro volcanic soil

Fig. 10. Change in grain size distribution during cyclic freeze-thawing (Ishikawa and Miura, 2011)

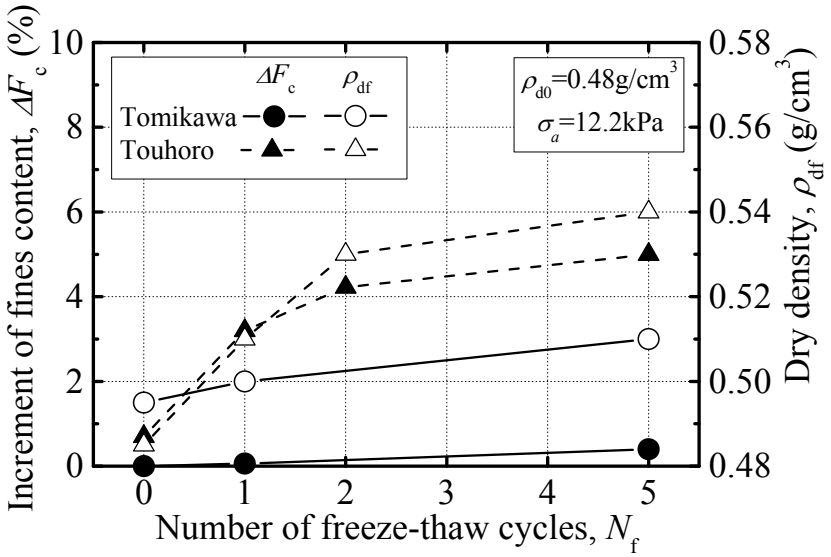

Fig. 11. Influence of freeze-thaw history on physical properties (Ishikawa and Miura, 2011)

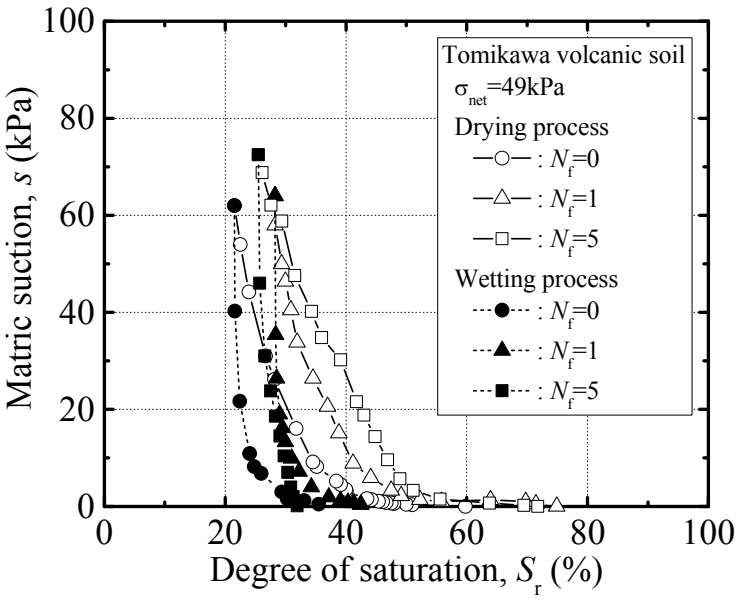

Fig. 12. Comparison of SWCCs for volcanic coarse-grained soil with different freeze-thaw histories

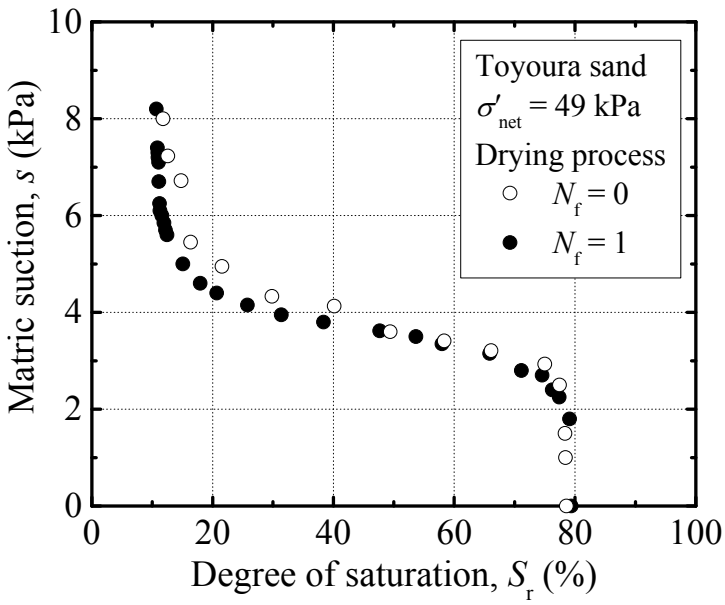

Fig. 13. Comparison of SWCCs for sand with different freeze-thaw histories

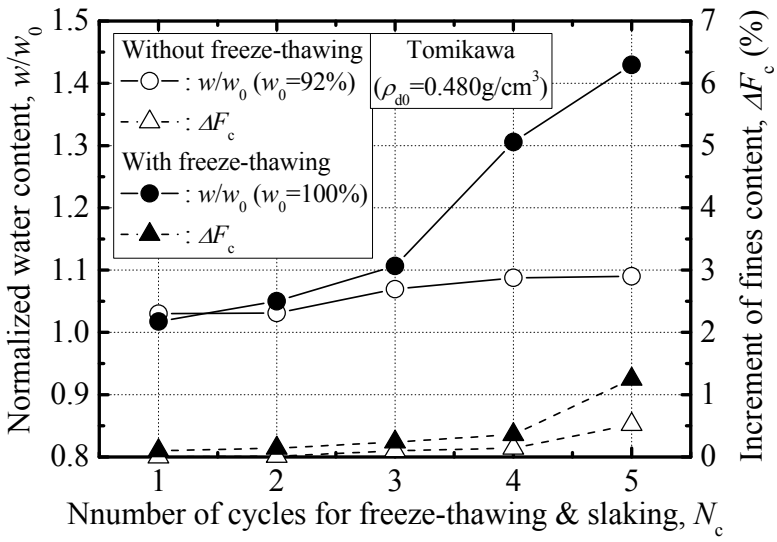

(a) Tomikawa volcanic soil

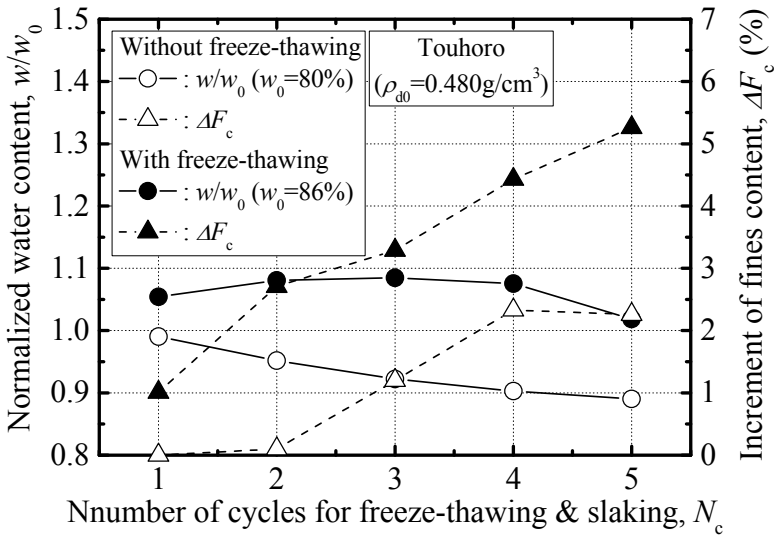

(b) Touhoro volcanic soil

Fig. 14. Change in water content and fines content with N_c

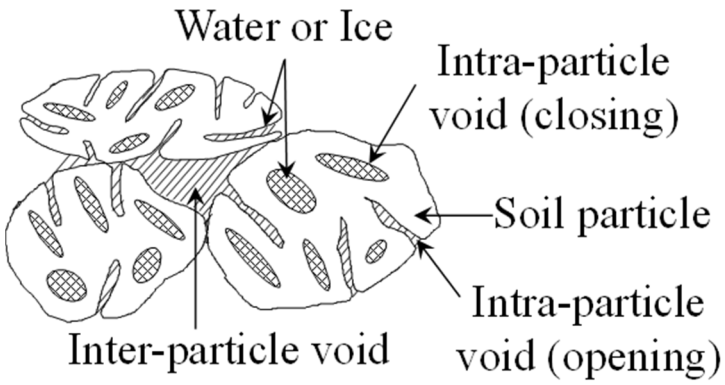

Fig. 15. Void structure for volcanic coarse-grained soil (after Nakata and Miura, 2007)

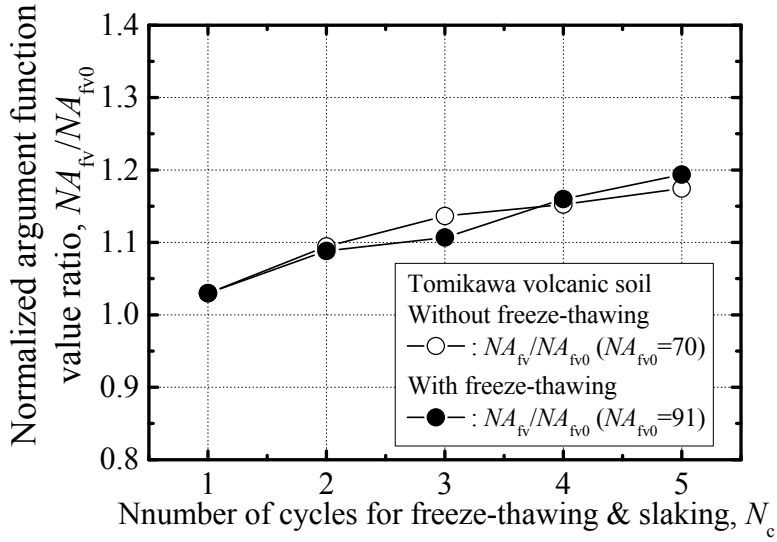

(a) Tomikawa volcanic soil

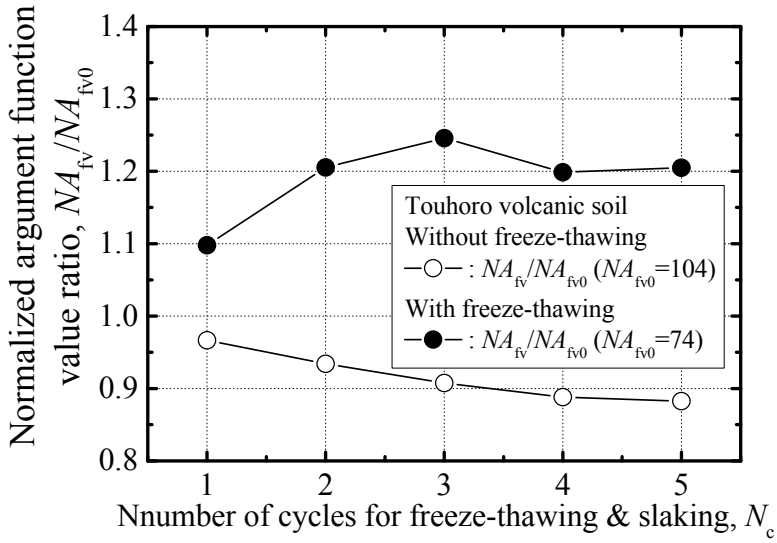

(b) Touhoro volcanic soil

Fig. 16. Change in particle shape with N_c.

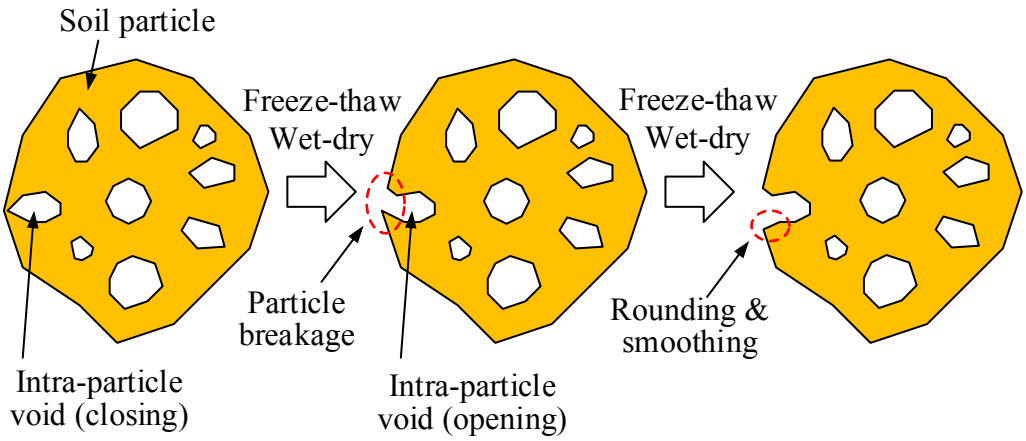

Fig. 17. Mechanism of particle shape change due to freeze-thaw actions and wet-dry cycles

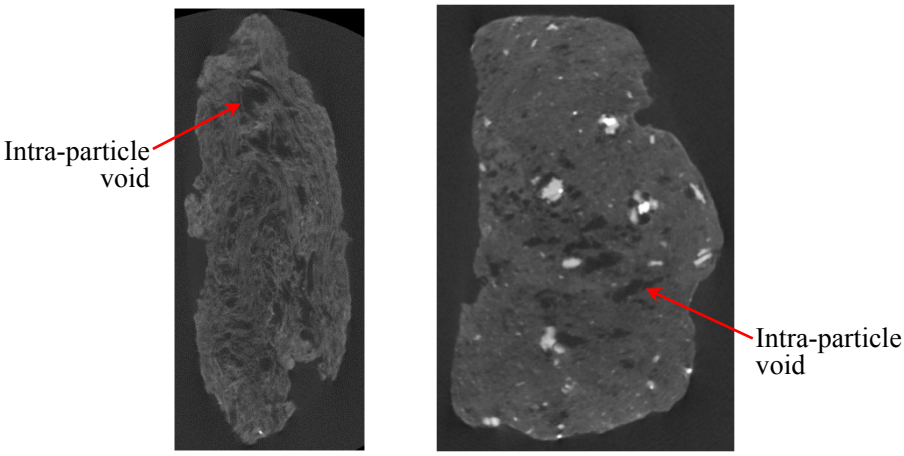

Fig. 18. X-ray CT observations for volcanic soil particles

(Left: Tomikawa volcanic soil, Right: Touhoro volcanic soil)

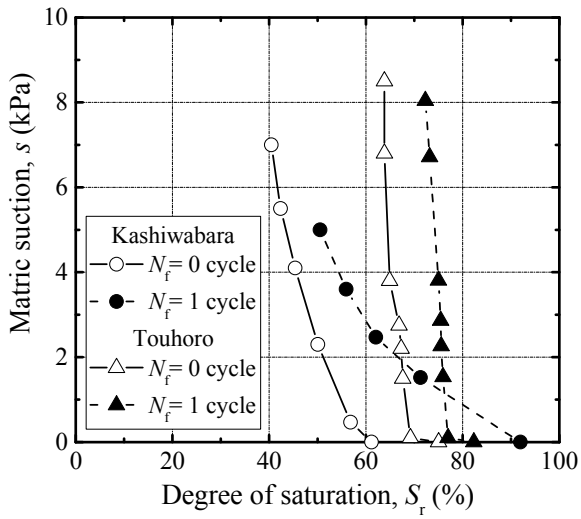

Fig. 19. Influence of freeze-thaw on water retentivity of volcanic coarse-grained soils

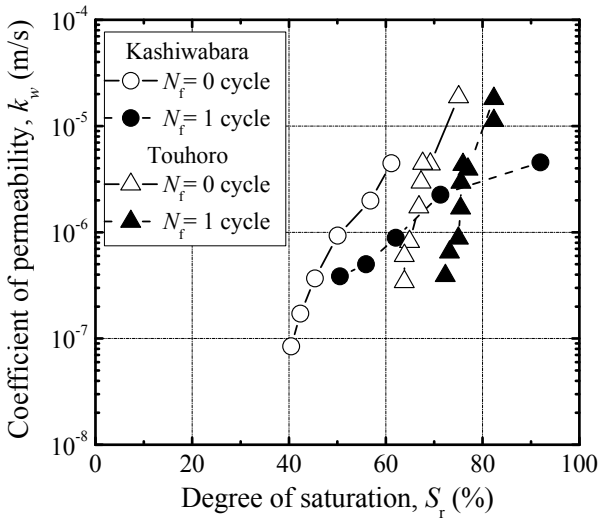

(a) k_w – S_r relations

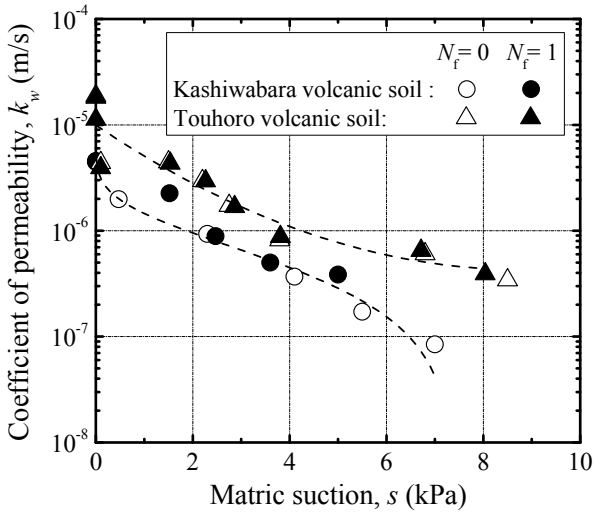

(b) k_w – s relations

Fig. 20. Influence of freeze-thaw on permeability of volcanic coarse-grained soils

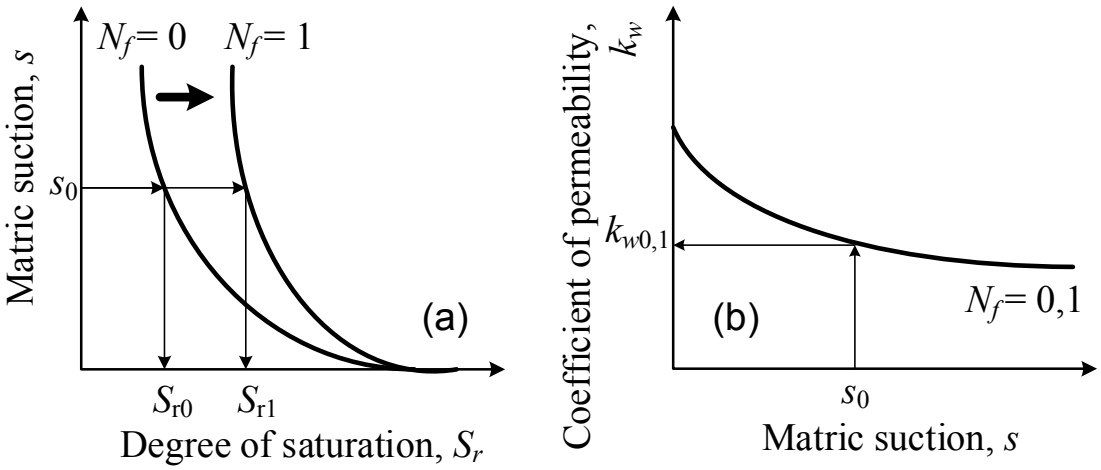

Fig. 21. Conceptional effects of freeze-thaw on (a) SWCC and (b) permeability